Computer Assisted Mechanics and Engineering Sciences, 10: 641–660, 2003.

Trefftz and RBF-based formulations for concrete beams analysis using damage models

Carlos M. Tiago*, Luís M.S.S. Castro**, Vitor M.A. Leitão***
DECivil-ICIST, Instituto Superior Técnico,
Av. Rovisco Pais, 1049-001 Lisboa, Portugal

(Received September 11, 2003)

In this work a hybrid-Trefftz formulation and a *meshless* approach based on the use of radial basis functions (RBF) are applied to the analysis of reinforced concrete beams. Resorting to the Mazars model, the concrete is represented by an elastic medium with progressive damage. In the hybrid-Trefftz formulation a stress field that satisfies *a priori* the equilibrium equations on the domain is used. The displacements on the static boundary are independently approximated, resulting in a governing system where the operators have to be integrated over the domain of the problem. In what concerns the *meshless* approach, radial basis functions are used to approximate the displacement fields but, as a collocation procedure is used, no integrations are required. A numerical example illustrates the results obtained with both techniques.

1. Introduction

The mesh requirements usually associated with traditional finite element methods may be diminished in, basically, two ways: by using boundary-type formulations (such as the BEM and, in a certain way, Trefftz techniques) or by establishing approximations based on nodes instead of based on elements (*meshless* methods).

The hybrid-stress Trefftz model used here is based on the direct approximation of the stress resultants using self-equilibrated and compatible states in the domain [1, 2]. This finite element model is similar to the one previously derived by Pereira [3]. From a structural engineering point of view, the main advantage of this numerical model when applied to the analysis of concrete structures is that locally equilibrated solutions are always obtained, ensuring then the conditions for the application of the static theorem of plasticity.

Several *meshless* methods have been devised in recent years, namely, the Smooth Particle Hydrodynamics [4], the Diffuse Approximation [5], the Reproducing Kernel Particle Methods [6], the Partition of Unity Method [7], the Element-Free Galerkin method [8], the *hp*-clouds Method [9] amongst others. Although the approximations are found without establishing a connection between nodes, some sort of background cell structure has to be used on most of them for domain integrations.

In this work a truly meshless approach, which totally avoids the need for a background cell structure (due to the use of the collocation approach and to the use of radial basis functions to build the global approximation), is used. Although relatively unknown, RBF collocation based approaches have been successfully applied in the solution of various partial differential equations problems [10–12].

*Assistant. E-mail: carlos.tiago@civil.ist.utl.pt. Tel: 351 21 841 82 64. Fax: 351 21 849 76 50.
**Auxiliary Professor. E-mail: luis@civil.ist.utl.pt. Tel: 351 21 841 82 53. Fax: 351 21 849 76 50.
***Associate Professor. E-mail: vitor@civil.ist.utl.pt. Tel: 351 21 841 82 34. Fax: 351 21 849 76 50.

The application to damage analysis of concrete beams is, in this work, carried out by using the Mazars model. This model was chosen basically due to its simplicity: a single variable is required to define the local damage and the number of material parameters is kept to a minimum. Numerical tests on a simply supported beam are presented and the results compared to other numerical and experimental ones available in the literature.

2. Reinforced concrete beams: formulation

2.1. Beam cross-section analysis

2.1.1. Strain

Using the Bernoulli hypothesis, the longitudinal strain at a given cross section is given by $\epsilon = \bar{\epsilon} + z\chi$, where χ and $\bar{\epsilon}$ are, respectively, the curvature and the longitudinal strain of the fibers over the origin of z axis. Assuming a constant distortion, κ, over the entire cross section, the following may be written

$$\boldsymbol{\epsilon} = \mathbf{E}\mathbf{e}, \tag{1}$$

where

$$\boldsymbol{\epsilon} = \begin{Bmatrix} \epsilon \\ \gamma \end{Bmatrix}, \quad \mathbf{E} = \begin{bmatrix} 1 & z & 0 \\ 0 & 0 & 1 \end{bmatrix} \quad \text{and} \quad \mathbf{e} = \begin{Bmatrix} \bar{\epsilon} \\ \chi \\ \kappa \end{Bmatrix}. \tag{2}$$

2.1.2. Stress

The generalised stresses in the section are defined by

$$\mathbf{s} = \int_{\Omega} \mathbf{E}^{\mathrm{T}} \boldsymbol{\sigma} \, \mathrm{d}\Omega, \tag{3}$$

where Ω is the cross sectional area of the beam and

$$\mathbf{s} = \begin{Bmatrix} N \\ M \\ V \end{Bmatrix} \quad \text{and} \quad \boldsymbol{\sigma} = \begin{Bmatrix} \sigma \\ \tau \end{Bmatrix}. \tag{4}$$

2.1.3. Constitutive relations

In the Mazars [13] model, the local damage is characterized by the scalar variable $0 < D < 1$. For the uniaxial case it takes the form

$$\sigma = (1 - D(\epsilon))E_0\epsilon, \tag{5}$$

where the damage variable, D, is a linear function of the basic variables, D_T and D_C, through the coefficients, α_T and α_C,

$$D(\epsilon) = \alpha_T D_T + \alpha_C D_C. \tag{6}$$

Assuming that the fibers are subjected to an uniaxial state of stress at all points, $\alpha_T = 1$ and $\alpha_C = 0$ for pure tension and $\alpha_T = 0$ and $\alpha_C = 1$ for pure compression.

The basic damage variables are given by

$$D_T(\epsilon) = 1 - \frac{\epsilon_{d0}(1-A_T)}{\widetilde{\epsilon}} - \frac{A_T}{e^{B_T(\widetilde{\epsilon}-\epsilon_{d0})}}; \qquad D_C(\epsilon) = 1 - \frac{\epsilon_{d0}(1-A_C)}{\widetilde{\epsilon}} - \frac{A_C}{e^{B_C(\widetilde{\epsilon}-\epsilon_{d0})}}, \tag{7}$$

where A_T, B_T, A_C and B_C are material dependent parameters, $\widetilde{\epsilon}$ is the equivalent strain and ϵ_{d0} is the maximum elastic strain.

The equivalent strain is given by

$$\widetilde{\epsilon} = \begin{cases} \epsilon & \text{if} \quad \epsilon \geq 0, \\ -\nu\sqrt{2}\epsilon & \text{if} \quad \epsilon < 0, \end{cases} \tag{8}$$

where ν is Poisson's ratio of the concrete. If $\widetilde{\epsilon} < \epsilon_{d0}$, then $D = 0$.

The rate relation of (5) is given by

$$\dot{\sigma} = (1 - D(\epsilon))E_0\dot{\epsilon} - \dot{D}E_0\epsilon, \tag{9}$$

with

$$\dot{D} = \mathcal{F}(\widetilde{\epsilon})\frac{\partial\widetilde{\epsilon}}{\partial\epsilon}\dot{\epsilon}, \tag{10}$$

where

$$\mathcal{F} = \alpha_T\mathcal{F}_T + \alpha_C\mathcal{F}_C \tag{11}$$

and

$$\mathcal{F}_T(\widetilde{\epsilon}) = \frac{\epsilon_{d0}(1-A_T)}{\widetilde{\epsilon}^2} + \frac{A_TB_T}{e^{B_T(\widetilde{\epsilon}-\epsilon_{d0})}}, \qquad \mathcal{F}_C(\widetilde{\epsilon}) = \frac{\epsilon_{d0}(1-A_C)}{\widetilde{\epsilon}^2} + \frac{A_CB_C}{e^{B_C(\widetilde{\epsilon}-\epsilon_{d0})}}. \tag{12}$$

For the reinforcement steel bars, a linear elastic relation is assumed,

$$\sigma_s = E_s\epsilon_s. \tag{13}$$

The constitutive relationship takes the form

$$\boldsymbol{\sigma} = \mathbf{C}\boldsymbol{\epsilon}, \tag{14}$$

where

$$\mathbf{C} = \begin{bmatrix} E(\epsilon)_{\text{mat}} & 0 \\ 0 & G \end{bmatrix}, \tag{15}$$

with

$$G = \frac{E(\epsilon)}{2(1+\nu)}; \qquad E(\epsilon)_{\text{mat}} = \begin{cases} (1 - D(\epsilon))\, E_0 & \text{if mat} = \text{concrete}, \\ E_s & \text{if mat} = \text{steel}. \end{cases}$$

Replacing (14) in definition (3) and taking into account both materials, concrete and steel, it is possible to write

$$\mathbf{s} = \int_\Omega \mathbf{E}^{\mathrm{T}}\mathbf{C}\boldsymbol{\epsilon}\,\mathrm{d}\Omega \;\Rightarrow\; \begin{Bmatrix} N \\ M \\ V \end{Bmatrix} = \begin{Bmatrix} b\displaystyle\int_{-h/2}^{h/2}(1 - D(\epsilon))\, E_0\, \epsilon\, \mathrm{d}z + E_s\sum_{i=1}^{n}\Omega s_i\, \epsilon_{s\,i} \\ b\displaystyle\int_{-h/2}^{h/2} z\,(1 - D(\epsilon))\, E_0\, \epsilon\, \mathrm{d}z + E_s\sum_{i=1}^{n} z_i\, \Omega s_i\, \epsilon_{s\,i} \\ b\displaystyle\int_{-h/2}^{h/2}(1 - D(\epsilon))\, G_0\, \gamma\, \mathrm{d}z \end{Bmatrix}, \tag{16}$$

where b and h are, respectively, the cross section's width and height, n is the number of reinforcement steel bars, Ωs_i is the cross sectional area of the i-th steel bar and z_i is the coordinate of the center of the i-th steel bar. It is important to remark that, for the sake of simplicity, only rectangular cross sections are being considered. However, the generalisation of the definitions and the equations presented here for other cross sections is straightforward [3].

Using definition (1), it is possible to rewrite (16) in the following matrix form

$$\mathbf{s} = \mathbf{k}\,\mathbf{e} \qquad \text{with} \qquad \mathbf{k} = \mathbf{k}_{\text{concrete}} + \mathbf{k}_{\text{steel}}, \tag{17}$$

with

$$\mathbf{k}_{\text{concrete}} = b \int_{-h/2}^{h/2} (1 - D(\epsilon)) \begin{bmatrix} E_0 & E_0\, z & 0 \\ E_0\, z & E_0\, z^2 & 0 \\ 0 & 0 & G_0 \end{bmatrix} \mathrm{d}z, \tag{18}$$

$$\mathbf{k}_{\text{steel}} = E_s \sum_{i=1}^{n} \begin{bmatrix} \Omega s_i & \Omega s_i\, z_i & 0 \\ \Omega s_i\, z_i & \Omega s_i\, z_i^2 & 0 \\ 0 & 0 & 0 \end{bmatrix}. \tag{19}$$

When the shear deformation is neglected, the third equation in (16) is no longer valid. In this case the shear stress resultant, V, may be recovered only by equilibrium conditions.

When an incremental analysis is to be implemented, it is necessary to write the constitutive relationship in the following form:

$$\mathbf{ds} = \mathbf{k}_T\,\mathbf{de} \quad \text{with} \quad \mathbf{k}_T = \begin{bmatrix} \dfrac{\partial N}{\partial \bar{\epsilon}} & \dfrac{\partial N}{\partial \chi} & \dfrac{\partial N}{\partial \kappa} \\ \dfrac{\partial M}{\partial \bar{\epsilon}} & \dfrac{\partial M}{\partial \chi} & \dfrac{\partial M}{\partial \kappa} \\ \dfrac{\partial V}{\partial \bar{\epsilon}} & \dfrac{\partial V}{\partial \chi} & \dfrac{\partial V}{\partial \kappa} \end{bmatrix}. \tag{20}$$

Finally, from (16) and (1) the following definition for the tangent stiffness matrix may be obtained:

$$\mathbf{k}_T = \mathbf{k}_{T\,\text{concrete}} + \mathbf{k}_{T\,\text{steel}} \tag{21}$$

with

$$\mathbf{k}_{T\,\text{concrete}} = b \int_{-h/2}^{h/2} \left((1 - D(\epsilon)) \begin{bmatrix} E_0 & E_0 z & 0 \\ E_0 z & E_0 z^2 & 0 \\ 0 & 0 & G_0 \end{bmatrix} - \frac{\partial\, D(\epsilon))}{\partial\, \epsilon} \begin{bmatrix} E_0 \epsilon & E_0 \epsilon z & 0 \\ E_0 \epsilon z & E_0 \epsilon z^2 & 0 \\ G_0 \gamma & G_0 \gamma z & 0 \end{bmatrix} \right) \mathrm{d}z, \tag{22}$$

$$\mathbf{k}_{T\,\text{steel}} = E_s \sum_{i=1}^{n} \begin{bmatrix} \Omega s_i & \Omega s_i\, z_i & 0 \\ \Omega s_i\, z_i & \Omega s_i\, z_i^2 & 0 \\ 0 & 0 & 0 \end{bmatrix}. \tag{23}$$

2.2. Beam analysis

This section summarises the relationships that characterizes the behaviour of the beam represented in Fig. 1.

2.2.1. Equilibrium equations

The equilibrium equations in the domain, in terms of the generalised stresses (or stress resultants), may be written as:

$$\mathbf{Ds} + \mathbf{f} = \mathbf{0} \quad \text{in} \quad (V) \tag{24}$$

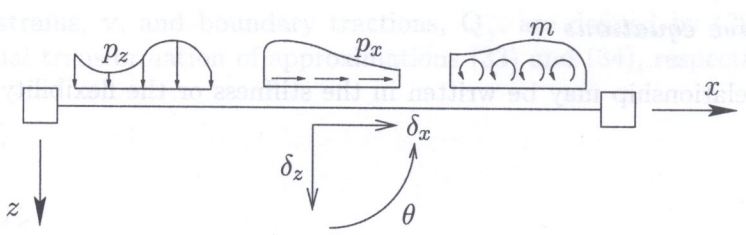

Fig. 1. Beam displacements and applied loads

where,

$$\mathbf{D} = \begin{bmatrix} \dfrac{\mathrm{d}}{\mathrm{d}x} & 0 & 0 \\ 0 & 0 & \dfrac{\mathrm{d}}{\mathrm{d}x} \\ 0 & \dfrac{\mathrm{d}}{\mathrm{d}x} & -1 \end{bmatrix} \quad \text{and} \quad \mathbf{f} = \begin{Bmatrix} p_x \\ p_z \\ m \end{Bmatrix}, \tag{25}$$

where p_x, p_z and m are, respectively, the longitudinal and transversal loads and the bending moment per unit length of the beam.

The static boundary conditions may be stated as follows:

$$\mathbf{N}\mathbf{s} = \mathbf{t}_\gamma \quad \text{on} \quad \Gamma_\sigma, \tag{26}$$

where matrix $\mathbf{N}$ collects the components of the unit outward normal vector and $\mathbf{t}_\gamma$ represents the applied forces, with

$$\mathbf{N} = \begin{bmatrix} n_x & 0 & 0 \\ 0 & 0 & n_x \\ 0 & n_x & 0 \end{bmatrix}. \tag{27}$$

2.2.2. Compatibility equations

The relationship between the generalized strains, $\mathbf{e}$, associated with the generalized stresses, $\mathbf{s}$, and the generalized displacements, $\boldsymbol{\delta}$, associated with the loads, $\mathbf{f}$, is obtained from the conjugated relation of (24)

$$\mathbf{e} = \mathbf{D}^*\boldsymbol{\delta} \quad \text{in} \quad (V) \tag{28}$$

with

$$\mathbf{D}^* = \begin{bmatrix} \dfrac{\mathrm{d}}{\mathrm{d}x} & 0 & 0 \\ 0 & 0 & \dfrac{\mathrm{d}}{\mathrm{d}x} \\ 0 & \dfrac{\mathrm{d}}{\mathrm{d}x} & 1 \end{bmatrix} \quad \text{and} \quad \boldsymbol{\delta} = \begin{Bmatrix} \delta_x \\ \delta_z \\ \theta \end{Bmatrix}, \tag{29}$$

where δ_x, δ_z and θ represent, respectively, the longitudinal and transversal displacements and the rotation. The kinematic boundary conditions may be stated as

$$\boldsymbol{\delta} = \boldsymbol{\delta}_\gamma \quad \text{on} \quad \Gamma_u, \tag{30}$$

where $\boldsymbol{\delta}_\gamma$ represents the prescribed displacements.

2.2.3. Constitutive equations

The constitutive relationship may be written in the stiffness or the flexibility forms, (17) or (31), respectively.

$$\mathbf{e} = \mathbf{k}^{-1}\mathbf{s} = \mathbf{f}\,\mathbf{s}. \tag{31}$$

When a linear elastic behaviour is assumed for the material, definition (18) leads directly to:

$$\mathbf{k}_{\text{concrete}} = \begin{bmatrix} E_0 A & 0 & 0 \\ 0 & E_0 I & 0 \\ 0 & 0 & G_0 A \end{bmatrix}; \qquad \mathbf{k}^{-1}_{\text{concrete}} = \begin{bmatrix} \dfrac{1}{E_0 A} & 0 & 0 \\ 0 & \dfrac{1}{E_0 I} & 0 \\ 0 & 0 & \dfrac{1}{G_0 A} \end{bmatrix}. \tag{32}$$

3. Hybrid–Trefftz stress model

In this section, the hybrid–Trefftz stress model is presented. For the sake of simplicity, the material will be assumed to exhibit linear elastic behaviour.

3.1. Approximation criteria

The hybrid-stress model [1] is based on the direct and independent approximation of the stress resultant field, $\mathbf{s}$, in the domain of each element and of the displacement field, $\boldsymbol{\delta}$, on the static boundary.

$$\mathbf{s} = \mathbf{S}_v\,\mathbf{X} + \mathbf{s}_p \qquad (V), \tag{33}$$

$$\boldsymbol{\delta} = \mathbf{U}_\gamma\,\mathbf{q}_\gamma \qquad (\Gamma_\sigma). \tag{34}$$

In Eqs. (33) and (34), matrices $\mathbf{S}_v$ and $\mathbf{U}_\gamma$ collect the approximation functions and vectors $\mathbf{X}$ and $\mathbf{q}_\gamma$ the corresponding weights. The vector $\mathbf{s}_p$ may be used to model particular solutions, such as body forces or residual stresses.

The columns of the approximation matrix $\mathbf{S}_v$ define linearly independent stress resultant fields induced by stress functions that solve the homogeneous Beltrami–Mitchell equations [1, 14]. Consequently, those stress resultant fields are self-equilibrated and are associated with elastic, compatible displacements, $\mathbf{U}_v$, that solve the homogeneous Navier equations,

$$(\mathbf{D}\,\mathbf{k}\,\mathbf{D}^*)\,\boldsymbol{\delta} + \mathbf{f} = \mathbf{0} \qquad (V).$$

It is then possible to verify [15] that:

$$\mathbf{D}\,\mathbf{S}_v = \mathbf{0}, \tag{35}$$

$$\mathbf{S}_v \quad = \mathbf{k}\,\mathbf{D}^*\mathbf{U}_v. \tag{36}$$

When body forces are applied in the domain of the element, the particular solution $\mathbf{s}_p$ is required to satisfy *a priori* the equilibrium equation

$$\mathbf{D}\,\mathbf{s}_p + \mathbf{f} = \mathbf{0} \quad \text{in} \quad (V), \tag{37}$$

and must also be associated with an elastic, compatible displacement field.

The generalised strains, $\mathbf{v}$, and boundary tractions, $\mathbf{Q}_\gamma$, are defined by (38) and (39), which correspond to the dual transformation of approximations (33) and (34), respectively.

$$\mathbf{v} = \int \mathbf{S}_v^t \, \mathbf{e} \, \mathrm{d}V, \tag{38}$$

$$\mathbf{Q}_\gamma = \int \mathbf{U}_\gamma^t \, \mathbf{t}_\gamma \, \mathrm{d}\Gamma_\sigma. \tag{39}$$

The above definitions are so chosen as to ensure that the pairs of discrete dual variables, $(\mathbf{X}, \mathbf{v})$ and $(\mathbf{q}_\gamma, \mathbf{Q}_\gamma)$ dissipate the same energy as the continuum fields they are used to represent.

In beam elements, the hybrid–Trefftz approximation (33) may be written in the following form:

$$\begin{bmatrix} N \\ M \\ V \end{bmatrix} = \begin{bmatrix} 0 & 0 & 1 \\ 1 - \dfrac{x}{L} & \dfrac{x}{L} & 0 \\ -\dfrac{1}{L} & \dfrac{1}{L} & 0 \end{bmatrix} \begin{bmatrix} X_1 \\ X_2 \\ X_3 \end{bmatrix} + \begin{bmatrix} n_0 \\ m_0 \\ v_0 \end{bmatrix}. \tag{40}$$

In can be easily verified that Eq. (36) leads to the following definition for matrix $\mathbf{U}_v$

$$\mathbf{U}_v = \begin{bmatrix} 0 & 0 & \dfrac{x}{E_0 A} \\ -\dfrac{x}{G_0 A L} - \dfrac{x^2}{2 E_0 I} + \dfrac{x^3}{6 E_0 I L} & \dfrac{x}{G_0 A L} - \dfrac{x^3}{6 E_0 I L} & 0 \\ \dfrac{x}{E_0 I} - \dfrac{x^2}{2 E_0 I L} & \dfrac{x^2}{2 E_0 I L} & 0 \end{bmatrix}. \tag{41}$$

The approximation of the displacement fields on the boundary of each beam element may be written in the following form

$$\begin{bmatrix} \delta_x \\ \delta_z \\ \theta \end{bmatrix}_{(x=0)} = \begin{bmatrix} 1 & 0 & 0 \\ 0 & 1 & 0 \\ 0 & 0 & 1 \end{bmatrix} \begin{bmatrix} q_1 \\ q_2 \\ q_3 \end{bmatrix}; \quad \begin{bmatrix} \delta_x \\ \delta_z \\ \theta \end{bmatrix}_{(x=L)} = \begin{bmatrix} 1 & 0 & 0 \\ 0 & 1 & 0 \\ 0 & 0 & 1 \end{bmatrix} \begin{bmatrix} q_4 \\ q_5 \\ q_6 \end{bmatrix}. \tag{42}$$

The nodal displacements q_i are identified in Fig. 2.

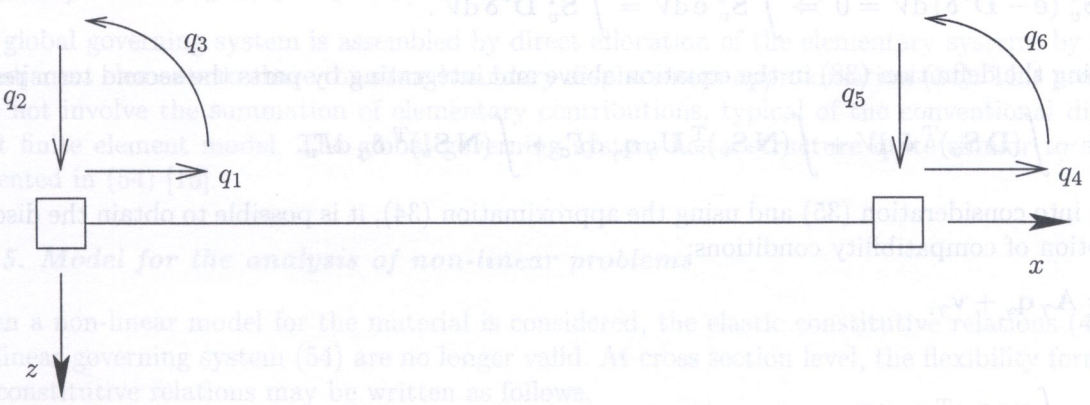

Fig. 2. Nodal displacements

3.2. Hybrid–Trefftz Stress Elements

3.2.1. Equilibrium

The hybrid–Trefftz approximation (33) ensures the equilibrium conditions in the domain *a priori*. The static boundary conditions are imposed in the following weighted residual form:

$$\int \mathbf{U}_\gamma^{\mathrm{T}} (\mathbf{N}\mathbf{s} - \mathbf{t}_\gamma)\, \mathrm{d}\Gamma_\sigma = 0.$$

Replacing in the previous equation the approximation (33), it is possible to verify that:

$$\int \mathbf{U}_\gamma^{\mathrm{T}} \mathbf{N}\mathbf{S}_v \mathbf{X}\, \mathrm{d}\Gamma_\sigma + \int \mathbf{U}_\gamma^{\mathrm{T}} \mathbf{N}\mathbf{s}_p\, \mathrm{d}\Gamma_\sigma = \int \mathbf{U}_\gamma^{\mathrm{T}} \mathbf{t}_\gamma\, \mathrm{d}\Gamma_\sigma.$$

The equilibrium conditions in the discrete model may then be written as follows:

$$\mathbf{A}_\gamma^{\mathrm{T}} \mathbf{X} = \mathbf{Q}_\gamma - \mathbf{Q}_{\gamma p}, \tag{43}$$

where

$$\mathbf{A}_\gamma = \int (\mathbf{N}\mathbf{S}_v)^{\mathrm{T}} \mathbf{U}_\gamma\, \mathrm{d}\Gamma_\sigma, \tag{44}$$

$$\mathbf{Q}_{\gamma p} = \int \mathbf{U}_\gamma^{\mathrm{T}} \mathbf{N}\, \mathbf{s}_p\, \mathrm{d}\Gamma_\sigma. \tag{45}$$

In the case of beam elements, matrix $\mathbf{A}_\gamma$ may be easily computed replacing definitions (40) and (42) in (44) to yield:

$$\mathbf{A}_\gamma = \begin{bmatrix} 0 & 0 & -1 \\ \dfrac{1}{L} & -\dfrac{1}{L} & 0 \\ -1 & 0 & 0 \\ 0 & 0 & 1 \\ -\dfrac{1}{L} & \dfrac{1}{L} & 0 \\ 0 & 1 & 0 \end{bmatrix}. \tag{46}$$

3.2.2. Compatibility

The weighted residual enforcement of the compatibility condition (28) may be written as follows:

$$\int \mathbf{S}_v^{\mathrm{T}} (\mathbf{e} - \mathbf{D}^* \boldsymbol{\delta})\, \mathrm{d}V = 0 \;\Rightarrow\; \int \mathbf{S}_v^{\mathrm{T}} \mathbf{e}\, \mathrm{d}V = \int \mathbf{S}_v^{\mathrm{T}} \mathbf{D}^* \boldsymbol{\delta}\, \mathrm{d}V\,.$$

Replacing the definition (38) in the equation above and integrating by parts the second term results

$$\mathbf{v} = -\int (\mathbf{D}\,\mathbf{S}_v)^{\mathrm{T}}\, \boldsymbol{\delta}\, \mathrm{d}V + \int (\mathbf{N}\,\mathbf{S}_v)^{\mathrm{T}}\, \mathbf{U}_\gamma\, \mathbf{q}_\gamma\, \mathrm{d}\Gamma_\sigma + \int (\mathbf{N}\,\mathbf{S}_v)^{\mathrm{T}}\, \boldsymbol{\delta}_\gamma\, \mathrm{d}\Gamma_u.$$

Taking into consideration (35) and using the approximation (34), it is possible to obtain the discrete description of compatibility conditions:

$$\mathbf{v} = \mathbf{A}_\gamma\, \mathbf{q}_\gamma + \mathbf{v}_\gamma, \tag{47}$$

where

$$\mathbf{v}_\gamma = \int (\mathbf{N}\,\mathbf{S}_v)^{\mathrm{T}}\, \boldsymbol{\delta}_\gamma\, \mathrm{d}\Gamma_u. \tag{48}$$

3.2.3. Elasticity conditions

Assuming linear elastic behaviour, the weighted residual enforcement of condition (31) leads to the following definition

$$\int \mathbf{S}_v^{\mathrm{T}}(\mathbf{e}-\mathbf{fs})\,\mathrm{d}V = 0 \;\Rightarrow\; \mathbf{v} = \int \mathbf{S}_v^{\mathrm{T}}\mathbf{f}\,\mathbf{S}_v\mathbf{X}\,\mathrm{d}V + \int \mathbf{S}_v^{\mathrm{T}}\mathbf{f}\mathbf{s}_p\,\mathrm{d}V.$$

The elasticity conditions in the discrete model may then be written in the form

$$\mathbf{v} = \mathbf{F}\mathbf{X} + \mathbf{v}_{pe}, \tag{49}$$

with

$$\mathbf{F} = \int \mathbf{S}_v^{\mathrm{T}}\,\mathbf{f}\,\mathbf{S}_v\,\mathrm{d}V, \tag{50}$$

$$\mathbf{v}_{pe} = \int \mathbf{S}_v^{\mathrm{T}}\,\mathbf{f}\,\mathbf{s}_p\,\mathrm{d}V. \tag{51}$$

Using Trefftz constraints, it is possible to obtain a boundary only integral expression for the flexibility matrix $\mathbf{F}$. Replacing definition (36) in (50) and integrating by parts to exploit condition (35), the following expression is found for matrix $\mathbf{F}$.

$$\mathbf{F} = \int \mathbf{U}_v^{\mathrm{T}}\,\mathbf{N}\,\mathbf{S}_v\,\mathrm{d}\Gamma. \tag{52}$$

The application of (52) to the beam element and neglecting the shear deformation ($GA = \infty$), leads to the usual definition:

$$\mathbf{F} = \begin{bmatrix} \dfrac{L}{3E_0I} & \dfrac{L}{6E_0I} & 0 \\ \dfrac{L}{6E_0I} & \dfrac{L}{3E_0I} & 0 \\ 0 & 0 & \dfrac{L}{E_0A} \end{bmatrix}. \tag{53}$$

3.2.4. Governing system

The elementary governing system (54) is obtained combining the discrete descriptions of equilibrium (43), compatibility (47) and elasticity (49).

$$\begin{bmatrix} \mathbf{F} & -\mathbf{A}_\gamma \\ -\mathbf{A}_\gamma^t & 0 \end{bmatrix} \begin{bmatrix} \mathbf{X} \\ \mathbf{q}_\gamma \end{bmatrix} = \begin{bmatrix} \mathbf{v}_\gamma - \mathbf{v}_{pe} \\ -\mathbf{Q}_\gamma + \mathbf{Q}_{\gamma p} \end{bmatrix}. \tag{54}$$

The global governing system is assembled by direct allocation of the elementary systems by requiring adjacent elements to share the same boundary displacement approximation (34). This procedure does not involve the summation of elementary contributions, typical of the conventional displacement finite element model. The global governing system has a structure quite similar to the one presented in (54) [15].

3.2.5. Model for the analysis of non-linear problems

When a non-linear model for the material is considered, the elastic constitutive relations (49) and the linear governing system (54) are no longer valid. At cross section level, the flexibility format for the constitutive relations may be written as follows,

$$\mathbf{e} = \mathbf{f}^*(\mathbf{s}), \tag{55}$$

where $\mathbf{f}^*(\mathbf{s})$ is a non-linear function depending on the current state of stress distribution.

The weighted residual enforcement of (55) leads to

$$\int \mathbf{S}_v^{\mathrm{T}} \left(\mathbf{e} - \mathbf{f}^*(\mathbf{s})\right) \mathrm{d}V = 0 \;\Rightarrow\; \mathbf{v} = \int \mathbf{S}_v^{\mathrm{T}}\, \mathbf{f}^*(\mathbf{s}),\, \mathrm{d}V. \tag{56}$$

The evaluation of the second term of (56) requires the use of a numerical integration scheme.

The non-linear governing system may now be written in the form:

$$\begin{cases} \displaystyle\int \mathbf{S}_v^{\mathrm{T}}\, \mathbf{f}^*(\mathbf{s}(\mathbf{X}))\, \mathrm{d}V - \mathbf{A}_\gamma\, \mathbf{q}_\gamma - \mathbf{v}_\gamma + \mathbf{v}_{pe} = \mathbf{0}, \\ -\mathbf{A}_\gamma^{\mathrm{T}}\, \mathbf{X} + \mathbf{Q}_\gamma - \mathbf{Q}_{\gamma p} = \mathbf{0}. \end{cases} \tag{57}$$

4. Hybrid–Trefftz implementation

In this section, the algorithms used in the physically non-linear analysis of concrete beams are described in detail. For the solution of the non-linear governing system (57) an incremental and iterative scheme based on the Newton-Raphson technique has been adopted. At the end of load step j, the current values of $\mathbf{X}_{(j)}$ and $\mathbf{q}_{\gamma\,(j)}$ satisfy the following equations:

$$\begin{cases} \displaystyle\int \mathbf{S}_v^{\mathrm{T}}\, \mathbf{f}^*(\mathbf{s}(\mathbf{X})_{(j)})\, \mathrm{d}V - \mathbf{A}_\gamma\, \mathbf{q}_{\gamma\,(j)} - \mathbf{v}_{\gamma\,(j)} + \mathbf{v}_{pe\,(j)} = \mathbf{0}, \\ -\mathbf{A}_\gamma^{\mathrm{T}}\, \mathbf{X}_{(j)} + \mathbf{Q}_{\gamma\,(j)} - \mathbf{Q}_{\gamma p\,(j)} = \mathbf{0}. \end{cases} \tag{58}$$

To obtain a solution for the next load increment, it is necessary to implement an iterative technique to compute the final values for $\mathbf{X}_{(j+1)}$ and $\mathbf{q}_{\gamma\,(j+1)}$. For initial solution we may use the results at the end of the previous load step, meaning that:

$$\mathbf{q}^0_{\gamma\,(j+1)} = \mathbf{q}_{\gamma\,(j)};\quad \mathbf{X}^0_{(j+1)} = \mathbf{X}_{(j)} \quad\Rightarrow\quad \mathbf{s}^0_{(j+1)} = \mathbf{s}_{(j)}. \tag{59}$$

At a given iteration, i, the residuals may be written as follows

$$\begin{cases} R_1(\mathbf{X}^i_{(j+1)}, \mathbf{q}^i_{\gamma\,(j+1)}) = \displaystyle\int \mathbf{S}_v^{\mathrm{T}}\, \mathbf{f}^*(\mathbf{s}(\mathbf{X})^i_{(j+1)})\, \mathrm{d}V - \mathbf{A}_\gamma\, \mathbf{q}^i_{\gamma\,(j+1)} - \mathbf{v}_{\gamma\,(j+1)} + \mathbf{v}_{pe\,(j+1)}, \\ R_2(\mathbf{X}^i_{(j+1)}) = -\mathbf{A}_\gamma^{\mathrm{T}}\, \mathbf{X}^i_{(j+1)} + \mathbf{Q}_{\gamma\,(j+1)} - \mathbf{Q}_{\gamma p\,(j+1)}. \end{cases} \tag{60}$$

Applying the Newton–Raphson technique, the correction terms $\Delta\mathbf{X}^i$ and $\Delta\mathbf{q}^i_\gamma$ result from the solution of system (61)

$$\begin{bmatrix} \dfrac{\partial R_1}{\partial \mathbf{X}} & \dfrac{\partial R_1}{\partial \mathbf{q}_\gamma} \\ \dfrac{\partial R_2}{\partial \mathbf{X}} & \dfrac{\partial R_2}{\partial \mathbf{q}_\gamma} \end{bmatrix}^i \begin{bmatrix} \Delta\mathbf{X} \\ \Delta\mathbf{q}_\gamma \end{bmatrix}^i = \begin{bmatrix} -R_1(\mathbf{X}^i_{(j+1)}) \\ -R_2(\mathbf{X}^i_{(j+1)}) \end{bmatrix}. \tag{61}$$

The derivatives involved in the definition of the Hessian matrix are defined by:

$$\frac{\partial R_1}{\partial \mathbf{X}} = \frac{\partial}{\partial \mathbf{X}} \left(\int \mathbf{S}_v^{\mathrm{T}}\, \mathbf{f}^*(\mathbf{s})\, \mathrm{d}V \right) = \int \mathbf{S}_v^{\mathrm{T}}\, \frac{\partial}{\partial \mathbf{s}}\, (\mathbf{f}^*(\mathbf{s}))\, \frac{\partial \mathbf{s}}{\partial \mathbf{X}}\, \mathrm{d}V = \int \mathbf{S}_v^{\mathrm{T}}\, \mathbf{k}_T^{-1}\, \mathbf{S}_v\, \mathrm{d}V, \tag{62}$$

$$\frac{\partial R_1}{\partial \mathbf{q}_\gamma} = -\mathbf{A}_\gamma\,; \quad \frac{\partial R_2}{\partial \mathbf{X}} = -\mathbf{A}_\gamma^{\mathrm{T}}\,; \quad \frac{\partial R_2}{\partial \mathbf{q}_\gamma} = \mathbf{0}. \tag{63}$$

Replacing (62) and (63) in (61), it is possible to obtain:

$$\begin{bmatrix} \int \mathbf{S}_v^{\mathrm{T}}\, \mathbf{k}_T^{-1}\, \mathbf{S}_v \, \mathrm{d}V & -\mathbf{A}_\gamma \\ -\mathbf{A}_\gamma^{\mathrm{T}} & 0 \end{bmatrix}^i \begin{bmatrix} \Delta \mathbf{X} \\ \Delta \mathbf{q}_\gamma \end{bmatrix}^i = \begin{bmatrix} -R_1(\mathbf{X}^i_{(j+1)}) \\ -R_2(\mathbf{X}^i_{(j+1)}) \end{bmatrix}. \tag{64}$$

The iterative correction of the variables $\mathbf{X}_{(j+1)}$ and $\mathbf{q}_{\gamma\,(j+1)}$ is ensured by the following equations

$$\mathbf{q}^{i+1}_{\gamma\,(j+1)} = \mathbf{q}^{i}_{\gamma\,(j+1)} + \Delta \mathbf{q}^i_\gamma \quad ; \quad \mathbf{X}^{i+1}_{(j+1)} = \mathbf{X}^i_{(j+1)} + \Delta \mathbf{X}^i. \tag{65}$$

For each load step, the iterative scheme here adopted may be summarised as follows:

1. Initialise variables: $\mathbf{q}^0_{\gamma\,(j+1)} = \mathbf{q}_{\gamma\,(j)}$; $\mathbf{X}^0_{(j+1)} = \mathbf{X}_{(j)}$; $R_1 = R_2 = 1$;
2. Evaluation of *load* quantities, $\mathbf{v}_{\gamma\,(j+1)}$, $\mathbf{v}_{pe\,(j+1)}$, $\mathbf{Q}_{\gamma\,(j+1)}$ and $\mathbf{Q}_{\gamma p\,(j+1)}$;
3. $iter = 0$
4. while $||R||_1 >$ TOL or $||R||_2 >$ TOL
   (a) Evaluate residual vectors, R_1 and R_2, using (60)
   (b) Evaluate Hessian Matrix in (64)
   (c) Solve linear system (64)
   (d) Update variables according to (65)
   (e) $iter = iter + 1$
5. End of the iterative procedure; $\mathbf{X}_{(j+1)} = \mathbf{X}^{iter}_{(j+1)}$, and $\mathbf{q}_{\gamma\,(j+1)} = \mathbf{q}^{iter}_{\gamma\,(j+1)}$

In the algorithm previously described, the evaluation of both integrals $\int_0^L \mathbf{S}_v^{\mathrm{T}}\, \mathbf{e}\, \mathrm{d}x$ and $\int_0^L \mathbf{S}_v^{\mathrm{T}}\, \mathbf{k}_T^{-1}\, \mathbf{S}_v\, \mathrm{d}x$ requires the use of numerical integration schemes. For this purpose, the Gauss-Lobatto quadrature rule [3] is used. It is possible to write:

$$\int_0^L \mathbf{S}_v^{\mathrm{T}}\, \mathbf{e}\, \mathrm{d}x = \int_{-1}^{1} \mathbf{S}_v^{\mathrm{T}}\, \mathbf{e}\, L/2\, \mathrm{d}\xi = \sum_{i=1}^{N_{\mathrm{Lob}}} \mathbf{S}\,(x(\xi_i))_v^{\mathrm{T}}\, \mathbf{e}_i\, w_i\, L/2, \tag{66}$$

$$\int_0^L \mathbf{S}_v^{\mathrm{T}}\, \mathbf{k}_T^{-1}\, \mathbf{S}_v\, \mathrm{d}x = \int_{-1}^{1} \mathbf{S}_v^{\mathrm{T}}\, \mathbf{k}_T^{-1}\, \mathbf{S}_v\, L/2\, \mathrm{d}\xi = \sum_{i=1}^{N_{\mathrm{Lob}}} \mathbf{S}\,(x(\xi_i))_v^{\mathrm{T}}\, \mathbf{k}_{T\,i}^{-1}\, \mathbf{S}\,(\xi_i)_v\, w_i\, L/2, \tag{67}$$

In (66) and (67), N_{Lob} denotes the number of Lobatto points used in the integration, ξ_i indicates the location of the i-th point and w_i stands for the corresponding weight.

In the implementation followed here, the shear deformation effect is neglected. This means that κ is always assumed to be zero and the definition for the tangent stiffness matrix has to be modified as follows

$$\mathbf{k}_T = \left[\begin{array}{cc|c} & & 0 \\ & \mathbf{k}_T^* & 0 \\ \hline 0 & 0 & \infty \end{array}\right] \quad \text{with} \quad \mathbf{k}_T^* = \begin{bmatrix} k_T^{(1,1)} & k_T^{(1,2)} \\ k_T^{(2,1)} & k_T^{(2,2)} \end{bmatrix}, \tag{68}$$

where $k_T^{(i,j)}$ is computed according to (22) and (23). The corresponding inverse, necessary to obtain the entries of the Hessian matrix, may be written as:

$$\mathbf{k}_T^{-1} = \left[\begin{array}{c|c} \mathbf{k}_T^{*\,-1} & \begin{matrix}0\\0\end{matrix} \\ \hline \begin{matrix}0 & 0\end{matrix} & 0 \end{array}\right]. \tag{69}$$

To compute (66) and (67) it is necessary to obtain the values of the generalised deformations $\mathbf{e}_i$ and the definition of the tangent stiffness matrices, $\mathbf{k}_{T\,i}$, for the cross sections with coordinates $x_i = (1+\xi_i)\,L/2$. The computation of these quantities requires the implementation of an iterative procedure. For each cross section, this algorithm may be stated as follows:

1. Compute the generalised stresses N and M using definition (40);
2. Initialise strains $\bar{\epsilon}_i^0 = \ldots$, $\chi^0 = \ldots$ and $R_N = R_M = 1.0$;
3. $iter = 0$
4. While $|R_N| > TOL$ or $|R_M| > TOL$;
   (a) Evaluate N_{calc}^{iter} and M_{calc}^{iter} replacing $\bar{\epsilon} = \bar{\epsilon}_i^{iter}$ and $\chi = \chi_i^{iter}$ in (17)
   (b) Evaluate k_T^* replacing $\bar{\epsilon} = \bar{\epsilon}_i^{iter}$ and $\chi = \chi_i^{iter}$ in (22) and (23)
   (c) $R_N = N_{calc}^{iter} - N$
   (d) $R_M = M_{calc}^{iter} - M$
   (e) Compute the Newton-Raphson correction

$$\left[\ \mathbf{k}_T^*\ \right]^{iter} \left[\begin{array}{c} \Delta\bar{\epsilon} \\ \Delta\chi_\gamma \end{array}\right]^{iter} = \left[\begin{array}{c} -R_N \\ -R_M \end{array}\right]$$

   (f) Update variables

$$\bar{\epsilon}^{\,iter+1} = \bar{\epsilon}^{\,iter} + \Delta\bar{\epsilon}^{iter} \quad \text{and} \quad \chi^{\,iter+1} = \chi^{\,iter} + \Delta\chi^{iter}$$

   (g) $iter = iter + 1$
5. End of the iterative procedure; $\mathbf{e}_i = \left[\begin{array}{c} \bar{\epsilon}^{iter} \\ \chi^{iter} \end{array}\right]$, and $\mathbf{k}_{T\,i} = \mathbf{k}_T^{iter}$

The computation of k_T^* is also performed using the Gauss–Lobatto's quadrature rule.

5. Radial Basis Functions with collocation

The main characteristic of the radial functions is that they exhibit radial symmetry: apart from the distance between the RBF center and a generic point, these functions depend only on some prescribed parameters. Their supports may be global or compact. In this work a globally supported RBF was used: the multiquadric (MQ) given by $\phi(\|x - x_j\|) = \sqrt{(x-x_j)^2 + c_j^2}$ where $c_j \neq 0$ is an adjustable local shape parameter.

Boundary value problems are, basically, solved by using weighted residuals techniques whereby an approximate solution is sought that best fits the governing equations and the boundary conditions

in the standard form:

$$\mathcal{L}u = \mathcal{F}, \tag{70}$$

where $\mathcal{L}^{\mathrm{T}} = [LI\ LB]$ collects the differential operators and $\mathcal{F}^{\mathrm{T}} = [FI\ FB]$ the prescribed values in the domain and boundary, respectively.

This fit may have a localized character (collocation) or a global one (or global in a certain region) in the way of Galerkin or other global forms of weighted residuals.

As what concerns collocation techniques using RBF two variants may be referred: asymmetrical or Kansa's collocation [10] and symmetrical collocation or collocation in the Hermite sense [11, 12].

5.1. Asymmetrical collocation

The interpolation of a given function (or data set), $s(x)$, using RBF, may be found in the following form:

$$s(x) = \sum_{j=1}^{N} \phi(\|x - x_j\|)\alpha_j, \tag{71}$$

where N is the number of radial basis functions used in the approximation.

The unknowns, α_j, are the weights of the radial basis functions. These may be obtained from the solution of the following system of equations, assuming the function is known at a given set of points, x_i:

$$s(x_i) = f(x_i) = \sum_{j=1}^{N} \alpha_j \phi(\|x_i - x_j\|). \tag{72}$$

The resulting system of equations is non-symmetrical and full. Some degree of sparsity may be added to the system if forms of domain decomposition are considered.

In some cases, it may be convenient to prescribe the function $s(x)$ at more points than strictly necessary resulting from this an overdetermined system of equations. In this last situation, a criteria has to be used to find the solution, e.g., the least-squares method.

The extension of this type of interpolation to boundary value problems is immediate. All is needed is to apply the (boundary and domain) differential operators to the previously defined approximation.

The following system may then be written:

$$LIu_h(x_i) = \sum_{k=1}^{N} \alpha_k LI\phi(\|x_i - \varepsilon_k\|), \tag{73}$$

$$LBu_h(x_i) = \sum_{k=1}^{N} \alpha_k LB\phi(\|x_i - \varepsilon_k\|). \tag{74}$$

5.2. Symmetrical collocation

The essence of the method consists in the application of the differential operators for each pair of collocation point-RBF center to an approximation that already takes into account the operators. By choosing points and centers to coincide a symmetrical system of equations arises.

The following approximation

$$u_h(x) = \sum_{k=1}^{N-M} \alpha_k LI_k^{\varepsilon}\phi(\|x - \varepsilon_k\|) + \sum_{k=N-M+1}^{N} \alpha_k LB_k^{\varepsilon}\phi(\|x - \varepsilon_k\|), \tag{75}$$

is used, where ε_k represents the center of the k RBF, $N-M$ is the number of RBF centers in the domain and M is the number of RBF centers in the boundary.

The equations obtained for the interior (domain) collocation points are

$$LI_j^x u_h(x_j) = \sum_{k=1}^{N-M} \alpha_k LI_j^x LI_k^\varepsilon \phi(\|x_j - \varepsilon_k\|) + \sum_{k=N-M+1}^{N} \alpha_k LI_j^x LB_k^\varepsilon \phi(\|x_j - \varepsilon_k\|), \tag{76}$$

and for the boundary collocation points one has

$$LB_j^x u_h(x_j) = \sum_{k=1}^{N-M} \alpha_k LB_j^x LI_k^\varepsilon \phi(\|x_j - \varepsilon_k\|) + \sum_{k=N-M+1}^{N} \alpha_k LB_j^x LB_k^\varepsilon \phi(\|x_j - \varepsilon_k\|), \tag{77}$$

where $L_j^x g(\|x-\varepsilon\|)$ is the function of ε obtained when L acts on $g(\|x-\varepsilon\|)$ as a function of x and then evaluated at $x = x_j$ and $L_k^\varepsilon g(\|x-\varepsilon\|)$ is the function of x, obtained when L acts on $g(\|x-\varepsilon\|)$ as a function of ε and then evaluated at $\varepsilon = \varepsilon_k$.

6. RBF IMPLEMENTATION

6.1. Irreducible form of the governing equations

In order to obtain a governing system of order as low as possible, a minimum number of variables should be approximated directly.

Neglecting the effect of shear deformation of the section, $\kappa = 0$, the compatibility Eqs. (28) take the form

$$\theta = -\frac{\mathrm{d}\delta_z}{\mathrm{d}x}; \qquad \bar{\epsilon} = \frac{\mathrm{d}\delta_x}{\mathrm{d}x}; \qquad \chi = -\frac{\mathrm{d}^2\delta_z}{\mathrm{d}x^2}. \tag{78}$$

Substituting this result in the elasticity relations (17) and assuming non-varying stiffness along the beam axis, the following definitions for the axial force and bending moment are obtained

$$N = k^{(1,1)}\frac{\mathrm{d}\delta_x}{\mathrm{d}x} + k^{(1,2)}\left(-\frac{\mathrm{d}^2\delta_z}{\mathrm{d}x^2}\right), \tag{79}$$

$$M = k^{(2,1)}\frac{\mathrm{d}\delta_x}{\mathrm{d}x} + k^{(2,2)}\left(-\frac{\mathrm{d}^2\delta_z}{\mathrm{d}x^2}\right), \tag{80}$$

where $k^{(i,j)}$ is the (i,j) element of the section stiffness matrix given by (17).

Substituting these results in the equilibrium equations yields for the shear force

$$V = k^{(2,1)}\frac{\mathrm{d}^2\delta_x}{\mathrm{d}x^2} + k^{(2,2)}\left(-\frac{\mathrm{d}^3\delta_z}{\mathrm{d}x^3}\right) + m, \tag{81}$$

and the two governing equations in the domain

$$k^{(1,1)}\frac{\mathrm{d}^2\delta_x}{\mathrm{d}x^2} + k^{(1,2)}\left(-\frac{\mathrm{d}^3\delta_z}{\mathrm{d}x^3}\right) + p_x = 0, \tag{82a}$$

$$k^{(2,1)}\frac{\mathrm{d}^3\delta_x}{\mathrm{d}x^3} + k^{(2,2)}\left(-\frac{\mathrm{d}^4\delta_z}{\mathrm{d}x^4}\right) + p_z = 0. \tag{82b}$$

The solution of the above equations requires three conditions to be imposed at each boundary point:

$$\delta_x = \overline{\delta}_x \quad \text{or} \quad N = \overline{N}, \tag{83a}$$

$$\delta_z = \overline{\delta}_z \quad \text{or} \quad V = \overline{V}, \tag{83b}$$

$$\theta = \overline{\theta} \quad \text{or} \quad M = \overline{M}, \tag{83c}$$

where N, V e M are given by (79), (81) e (80) and "—" stands for prescribed quantity on the boundary. If the domain is decomposed into several regions, then appropriate continuity conditions are required:

$$\delta_x^i - \delta_x^{ii} = 0, \tag{84a}$$

$$\delta_z^i - \delta_z^{ii} = 0, \tag{84b}$$

$$\theta^i - \theta^{ii} = 0, \tag{84c}$$

$$N^i - N^{ii} = \overline{N}_I, \tag{84d}$$

$$V^i - V^{ii} = \overline{V}_I, \tag{84e}$$

$$M^i - M^{ii} = \overline{M}_I, \tag{84f}$$

$$\tag{84g}$$

where the indexes i and ii identify the cross sections of two contiguous regions and $\overline{N}_I$, $\overline{V}_I$ and $\overline{M}_I$ represent concentrated loads at interface I.

6.2. Governing system

A numerical solution to the problem defined by Eqs. (82), (83) and (84) may be found, as stated before, by the use of asymmetrical collocation. In this case, the variables are approximated as follows:

$$\delta_x(x) = \sum_{i=1}^{N_{\delta_x}} \alpha_i^{\delta_x} \phi(\|x - x_i\|), \qquad \delta_z(x) = \sum_{i=1}^{N_{\delta_z}} \alpha_i^{\delta_z} \phi(\|x - x_i\|), \tag{85}$$

where x_i represents the coordinates of the RBF points, N_{δ_x} and N_{δ_z} are the number of RBF used to approximate each component of the displacement field.

In order to rewrite the problem in the form presented earlier (70), the domain and boundary differential operators take the following definitions, respectively:

$$LI = \begin{bmatrix} k^{(1,1)} \dfrac{\mathrm{d}^2}{\mathrm{d}x^2} & k^{(1,2)} \left(-\dfrac{\mathrm{d}^3}{\mathrm{d}x^3} \right) \\ k^{(2,1)} \dfrac{\mathrm{d}^3}{\mathrm{d}x^3} & k^{(2,2)} \left(-\dfrac{\mathrm{d}^4}{\mathrm{d}x^4} \right) \end{bmatrix}, \tag{86}$$

and

$$LB = \begin{bmatrix} 1 & 0 \\ 0 & 1 \\ 0 & -\dfrac{\mathrm{d}}{\mathrm{d}x} \\ k^{(1,1)} \dfrac{\mathrm{d}}{\mathrm{d}x} & k^{(1,2)} \left(-\dfrac{\mathrm{d}^2}{\mathrm{d}x^2} \right) \\ k^{(2,1)} \dfrac{\mathrm{d}^2}{\mathrm{d}x^2} & k^{(2,2)} \left(-\dfrac{\mathrm{d}^3}{\mathrm{d}x^3} \right) \\ k^{(2,1)} \dfrac{\mathrm{d}}{\mathrm{d}x} & k^{(2,2)} \left(-\dfrac{\mathrm{d}^2}{\mathrm{d}x^2} \right) \end{bmatrix}. \tag{87}$$

Similarly way, the vector of the unknowns and the right-hand side vector are:

$$u^t = \begin{bmatrix} \delta_x & \delta_z \end{bmatrix}, \tag{88}$$

and

$$FI^t = \begin{Bmatrix} p_x & p_z \end{Bmatrix}, \qquad FB^t = \begin{Bmatrix} \overline{\delta}_x & \overline{\delta}_z & \overline{\theta} & \overline{N} & \overline{V} & \overline{M} \end{Bmatrix}, \tag{89}$$

for domain and the boundary, respectively. For simplicity, the continuity conditions have been omitted in the above definitions.

The application of the operators to the approximation (71) used in this work (the same could have been done for approximation (75), that is, the symmetrical form) requires several derivatives to be computed. In this work all derivatives were carried out symbolically with the use of MATLAB [16] rendering quite simple the task of determining the entries of the system of equations:

$$\mathbf{A}\boldsymbol{\alpha} = \mathcal{F}. \tag{90}$$

If the number of collocation points is chosen in such a way that the governing system matrix is square, then the solution will satisfy exactly all the boundary and continuity conditions and the compatibility equations in the domain. The equilibrium equations will be satisfied only at the collocation points.

6.3. Implementation

Similarly to the hybrid–Trefftz implementation, an incremental and iterative procedure had to be devised. In this implementation, the secant method was used to solve the non-linear problem. The incremental form of (90) can be written as

$$\mathbf{A}_{\text{sec}}\Delta\boldsymbol{\alpha} = \Delta\mathcal{F}, \tag{91}$$

where $\mathbf{A}_{\text{sec}}$ is the system matrix evaluated using the section stiffness matrix given by (17), which is equal to the first term of the $\mathbf{k}_{T\,\text{concrete}}$ given by (22).

The algorithm is the following:

1. Compute, for a given number of collocation points in the domain, the number of required RBF centers and the associated coordinates;
2. Form the vector $\Delta\mathcal{F}$ of the parametric load, given by $\Delta\mathcal{F}^{\mathrm{T}} = [FI\ FB]$;
3. Initialize the unknowns vector, $\boldsymbol{\alpha}_0 = \mathbf{0}$;
4. Initialize the stiffness matrix of each cross section at the collocation points, given by (17). As $\boldsymbol{\alpha}_0 = \mathbf{0}$, at all collocation points $\mathbf{e} = \mathbf{0}$ and $D = 0$;
5. **Incremental process:** FOR inc=1:number of increments;
   (a) set the residual vector $\psi = \Delta\mathcal{F}$;
   (b) **iterative process:** WHILE $\psi > TOL$;
      i. FOR all collocation points: compute the deformations $\mathbf{e}$ and the stiffness matrix of the section given by (17).
      ii. Compute the system matrix;
      iii. Solve the resulting system of Eqs. (90);
      iv. Update the solution, $\boldsymbol{\alpha} = \boldsymbol{\alpha} + \Delta\boldsymbol{\alpha}$;
      v. Compute the updated residual vector, ψ;

The integration of the constitutive relationship (17) is achieved by using Gauss–Lobatto quadrature rule.

7. Numerical example

Consider the simplified model of a simply supported beam with a rectangular cross section presented in Fig. 3. The axis origin is located at the geometric center of the cross section.

The concrete parameters for the Mazars damage model (wich were found experimentally [17]) are the following: $A_T = 0.995$, $B_T = 8000$, $A_C = 0.85$, $B_C = 1050$, $\epsilon_{d0} = 0.00007$, $E_0 = 29200 \cdot 10^6$ Pa

and $\nu = 0.2$. The stress-strain curve associated with these parameters is plotted in Fig. 4a. The corresponding damage-strain curve is indicated in Fig. 4b. For the steel reinforcement, the following data is assumed: elasticity modulus $E_s = 196000 \cdot 10^6$ Pa, tensile steel area $A_{st} = 3 \times \pi \times 0.01^2/4$ m^2 with 0.02 m concrete cover, compressive steel area $A_{sc} = 2 \times \pi \times 0.005^2/4$ m^2 with 0.015 m concrete cover. In the analysis of this structure with the hybrid–Trefftz model, two elements are considered. A total of 12 discrete variables are involved in the approximation; 6 generalised stresses, $\mathbf{X}$, and 6 nodal displacements, $\mathbf{q}_\gamma$. The load was applied in 10 increments of 4 kN each. For the numerical integrations defined over the cross section and along the bar, 10 Lobatto points have been considered. The numerical model used here was implemented in MATLAB [16] environment.

In the analysis carried out with the RBF implementation, and to ensure a correct modelling of the point load, the domain was also divided into two subregions, with the interface at the cross section where the load is applied. In this example, a total of 44 unknowns (corresponding to the use of 8 radial basis for each component of the displacement field in each of the two regions) was considered. The values used for the parameter c_j in the multiquadric RBF were: $c_j = 1.0$ for the first region (between the left support and the concentrated load) and $c_j = 0.6$ on the second region (between the concentrated load and the right end of the beam). Ten Gauss–Lobatto points were used to integrate the constitutive relations (17). The load increment was equal to 2.25 kN.

The load-displacement diagram obtained with both numerical schemes is plotted in Fig. 5. In this diagram, the evolution of the load is plotted against the value of the transversal displacement measured at the end of the beam, $x = 1.2$ m. In the same figure, the results obtained with an *hp*-cloud implementation [18] are also presented. It is possible to verify that all these numerical results are quite similar and are quite close to the experimental measurements described in [17].

Figure 6 correspond to the solution obtained with the hybrid–Trefftz approach and shows several contours obtained at the end of the loading process for the damage variable. A negative value in this plot means the damage occurs due compression.

Figure 7 shows the damage distribution at the end of each load step considered in the analysis.

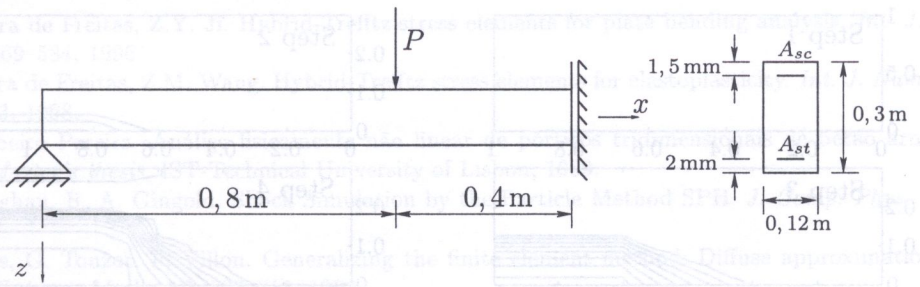

Fig. 3. Beam: geometry and boundary conditions

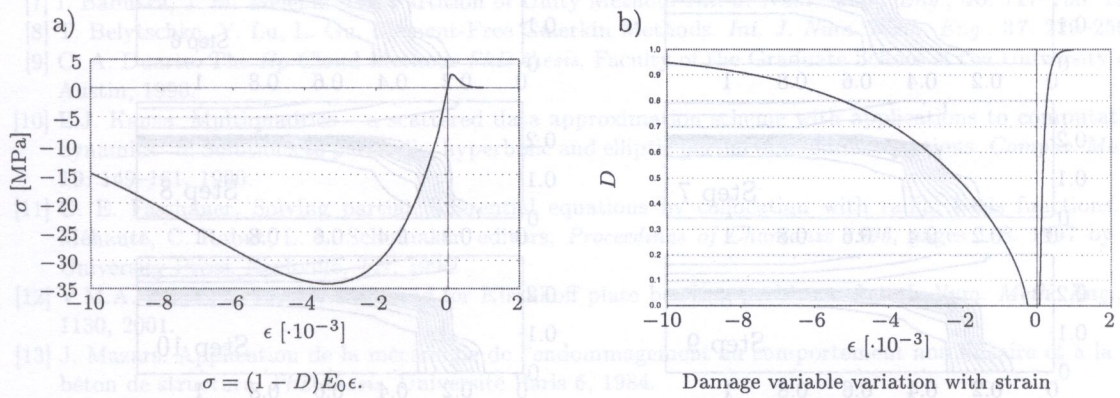

Fig. 4. Constitutive relation of the concrete for the Mazars damage model

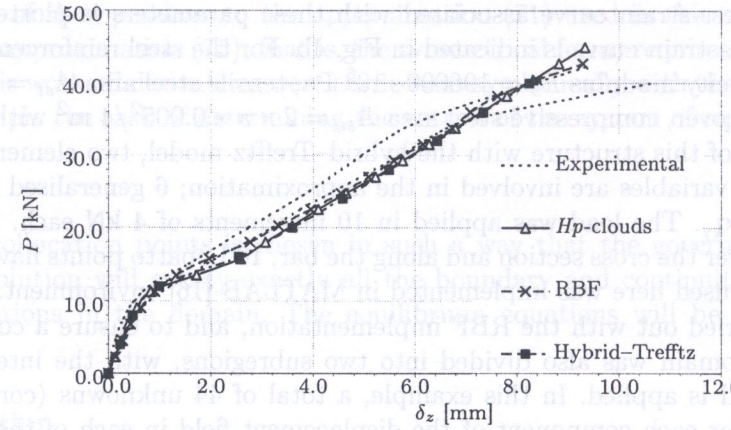

Fig. 5. Load-displacement diagrams

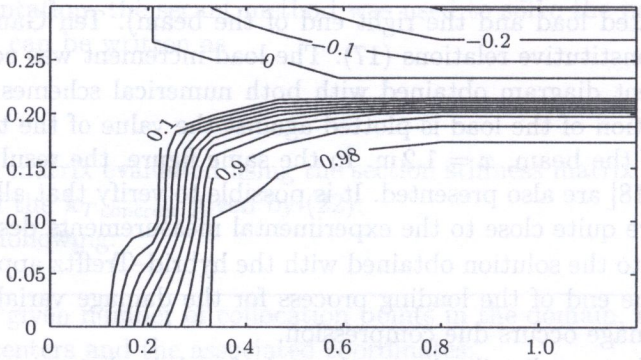

Fig. 6. Damage distribution of the solution obtained with the Trefftz model

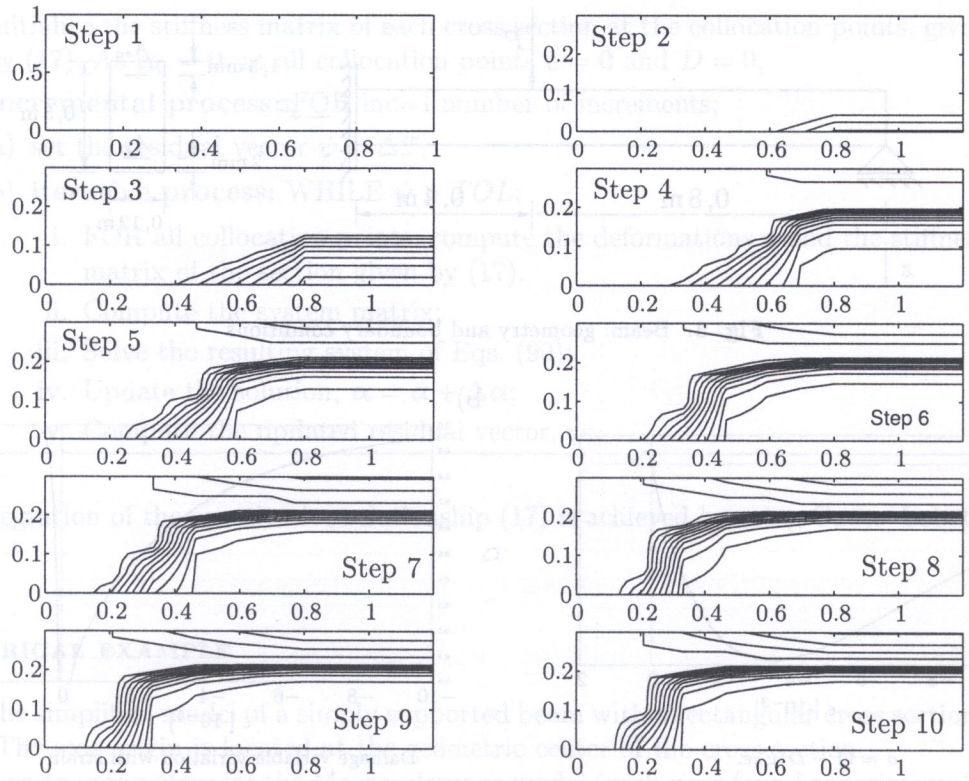

Fig. 7. Evolution of the damage distribution in the Trefftz model

8. Conclusions

In this work, applications of a meshless collocation technique based on radial basis functions and of a hybrid-Trefftz technique to the analysis of a non-linear structural problem were presented and assessed.

The non-linearity of the constitutive relationship assumed for the concrete, the damage model of Mazars, requires the use of an incremental and iterative scheme and this is basically what presented more difficulties in terms of implementation (when compared to a linear problem). Due to the particular aspects of each formulation (displacements are approximated in the RBF approach whereas generalised stresses are approximated in the hybrid-Trefftz technique), two inherently different incremental and iterative approaches were implemented.

The results obtained with both techniques are similar to the experimental ones and other numerical studies (the *Hp*-clouds method) available in the literature which further confirms the possibility of using both techniques as tools to study the behavior of this type of non-linear structural problems.

It may be referred that the RBF technique is slightly easier to implement than the Trefftz technique but it should also be stated that the mathematical foundations of the Trefftz technique are, at this stage, more sound than the RBF technique in what concerns (mathematical) proofs of convergence and stability.

9. Acknowledgments

This work has been partially supported by FCT through projects "Financiamento Plurianual" and POCTI/33066/ECM/2000. The authors wish to thank Dr. Sérgio Proença for his help and support and Mrs. Cristina Silva for her help in the implementation of the Trefftz model.

References

[1] J.A. Teixeira de Freitas, Z.Y. Ji. Hybrid-Trefftz stress elements for plate bending analysis. *Int. J. Num. Meth. Eng.*, **39**: 569–584, 1996.

[2] J.A. Teixeira de Freitas, Z.M. Wang. Hybrid-Trefftz stress elements for elastoplasticity. *Int. J. Num. Meth. Eng.*, **43**: 655–683, 1998.

[3] E.M.B. Ribeiro Pereira. Análise fisicamente não linear de pórticos tridimensionais de betão armado (in portuguese). *Master's thesis*, IST-Technical University of Lisbon, 1989.

[4] J. J. Monaghan, R. A. Gingold. Shock Simulation by the Particle Method SPH. *J. Comp. Phys.*, **52**: 374–389, 1983.

[5] B. Nayroles, G. Touzot, P. Villon. Generalizing the finite element method: Diffuse approximation and diffuse elements. *Comput. Mech.*, **10**: 307–318, 1992.

[6] W. K. Liu, Y. Chen, S. Jun, J. S., T. Belytschko, C. Pan, R. A. Uras, C. T. Chang. Overview and applications of the Reproducing Kernel Particle Methods. *Arch. of Comput. Meth. in Eng.*, **3**(1): 3–80, 1996.

[7] I. Babuška, J. M. Melenk. The Partition of Unity Method. *Int. J. Num. Meth. Eng.*, **40**: 727–758, 1997.

[8] T. Belytschko, Y. Lu, L. Gu. Element-Free Galerkin Methods. *Int. J. Num. Meth. Eng.*, **37**: 229–256, 1994.

[9] C. A. Duarte. The *Hp* Cloud Method. *PhD thesis*, Faculty of the Graduate School of the University of Texas at Austin, 1996.

[10] E.J. Kansa. Multiquadrics – a scattered data approximation scheme with applications to computational fluid-dynamics - ii: Solutions to parabolic, hyperbolic and elliptic partial differential equations. *Comput. Math. Applic.*, **19**: 149–161, 1990.

[11] G. E. Fasshauer. Solving partial differential equations by collocation with radial basis functions. In: A. Le Méhauté, C. Rabut, L. L. Schumaker, editors, *Proceedings of Chamonix 1996*, pages 1–8. 1997 by Vanderbilt University Press, Nashville, TN, 1996.

[12] V.M.A. Leitão. A meshless method for Kirchhoff plate bending problems. *Int. J. Num. Meth. Eng.*, **52**: 1107–1130, 2001.

[13] J. Mazars. Application de la mécanique de l'endommagement au comportement non lineaire et à la rupture du béton de structure. *PhD thesis*, Université Paris 6, 1984.

[14] J.A. Teixeira de Freitas, Z.Y. Ji. Hybrid-trefftz boundary integral formulation for simulation of singular stress fields. *Int. J. Num. Meth. Eng.*, **39**: 281–308, 1996.

[15] J.A. Teixeira de Freitas, J.P. Moitinho de Almeida, E.M.B. Ribeiro Pereira. Non-conventional formulations for the finite element method. *Comput. Mech.*, **23**(5-6): 488–501, 1999.

[16] The MathWorks Inc. *MATLAB, The Language of Technical Computing.* Version 6.0, 2000.

[17] M. S. Álvares. Estudo de um modelo de dano para o concreto: formulação, identificação paramétrica e aplicação com o emprego do método dos elementos finitos (in portuguese). *Master's thesis*, Escola de Engenharia de São Carlos, Universidade de São Paulo, 1993.

[18] F. B. Barros. Métodos Sem Malha e Método dos Elementos Finitos Generalizados em Análise Não-Linear de Estruturas (in portuguese). *PhD thesis*, Escola de Engenharia de São Carlos, Universidade de São Paulo, 2002.